IADC/SPE-208729-MS

Real-Time Drilling Bit Fault and Symptom Diagnosis During Operation Based on Cutter Force Modeling of PDC Polycrystalline Diamond Compact Bits

Mostafa Gomar and Behzad Elahifar, Norwegian University of Science and Technology

This paper was prepared for presentation at the IADC/SPE International Drilling Conference and Exhibition held in Galveston, Texas, USA, 8–10 March 2022.

Abstract

Wired drillpipe with along string measurement sensors is a key to drilling events prediction. An interesting objective during drilling operations is real-time assessment of the drill bit to determine an acceptable time to stop drilling and change the drill bit. In addition, dynamic modeling of the drillstring requires the calculation of forces at the bit. A novel approach to deal with this challenge involved experiments and the evaluation of the forces on the cutters based on their geometrical characteristics, rock, and drilling parameters.

In this research two empirical correlations were developed based on the experimental data from numerous works to evaluate normal and contact forces on polycrystalline diamond compact (PDC) cutters. More than 700 data points were collected and utilized to investigate the influence of parameters such as differential pressure, cutter size, cut depth, cutter wear state, rock drillability, and back rake angle on the normal and contact forces on cutters. Machine learning techniques such as deep learning, nonlinear regression approaches, and genetic algorithms were implemented to fit nonlinear equations to data points.

The outcome of this research (cutter-force equations) could be utilized to determine normal, lateral, and tangential forces on PDC cutters as inputs and constraints to model drillstring dynamics. Besides, the models could be adopted as a measure to assess bit conditions in real-time drilling and predict drilling events and issues related to the bit and mitigate drawbacks before they occur.

All available correlations and equations concerning cutter-rock interaction only consider one or two parameters or are just applicable under atmospheric conditions. The novelty of this research revolves around developing thorough cutter-force models to include all design and operational parameters under real differential fluid pressure.

Introduction

Real-time and post-drilling assessment of polycrystalline diamond compact (PDC) bits requires knowledge of the interaction between cutters and rock. Such studies should comprise the forces and stresses on the cutters; otherwise, much of the instant and important local effects during rock cutting would be lost during drilling. Furthermore, the study of the drillstring dynamics which considers torsional vibration should

incorporate an accurate bit-rock interaction law. The value and spatial distribution of stresses on cutters depend on the applied drilling parameters (torque on bit, weight on bit, rotary speed, and hydraulic forces) and design characteristics of PDC bits (rake angles, bit profile, cutter size, and cutter distribution, wear flat area, and chamfer angle).

Single cutter testing, compared to full-scale testing, introduces more insights into studying cutter-rock interaction and the dynamics of rock-bit interaction. Single cutter testing is more versatile than full-scale testing if the objective is to accurately control both the operating conditions and the simulated downhole conditions during a cutting test (Zijsling 1987). A lot of experimental and theoretical research has been done to introduce reliable cutter-rock interaction models. Glowka (1989) performed an extensive experimental and theoretical study to implement single cutter force concepts in the analysis of PDC bit design in geothermal applications. The examinations suggested a strong dependence of the PDC cutter wear rate on the frictional temperature, the abrasiveness of the rock, and the stresses that develop at the cutter-rock interface. Detournay and Defournay (1992) developed a phenomenological model to study the drilling response of drag bits based on cutter-rock interaction forces and verified the model using experimental data. Subsequently, Dagrain et al. (2001) modified the same concept to investigate the influence of the cutter geometry on the forces acting on a cutter. A complementary model to the above research was introduced to probe the drilling response of drag bits and provide the relationship between the weight on bit, the torque on bit, the rate of penetration, and the angular velocity (Detournay et al. 2008).

Generally, most of the research relating to cutter-rock interaction revolves around investigating the influence of confining pressure, cutter geometry design parameters (back rake and side rake angles), cutting area and wear height, and rock drillability.

Confining pressure. One of the promising factors during drilling in porous media is the effect of the confining pressure or dynamic pore pressure on the forces and stresses distributed within the rock by cutter action. Experimental data on the single cutter test have proved that there is a significant increase in mechanical specific energy even at low confining pressures and with permeable rocks (Rafatian et al. 2015, Rajabov et al. 2012). As long as the rock undergoes stress distribution, pore pressure inside the rock could be affected by the mechanical stresses under poroelastic laws (Rafatian et al. 2015, Chen et al. 2018). Furthermore, the mechanical properties of the crushed rock ahead of cutters could affect the required force during drilling (Ledgerwood 2007). Besides, in absence of any cleaning practice of cutters by drilling fluid, the amount of energy dissipated due to the friction of cutting on the cutter surface has significant value compared to intrinsic specific energy (Chen et al. 2018). Further studies demonstrate the effect of confining pressure on the cutting action of a single cutter and drilling process and all of them have shown significant influence of fluid pressure on specific energy, stresses, and the mode of cutting removal ahead of bit (Detournay and Atkinson 2000, Zijsling 1987, Grima et al. 2015, Akbari et al. 2014, Ledgerwood 2007). The result from experiments by Rafatian et al. (2015) validated a nonlinear relationship at low confining pressure up to*150 psi*. In this study, correlations are developed by considering positive confining pressure (i.e., wellbore pressure greater than pore pressure).

Cutter geometry design parameter (Back rake and side rake angles). Many investigations have indicated that the number of forces (vertical and cutting forces) applied for cutting the rock are at a minimum at the back rake angle around *15°* (Liang et al. 2014, Rajabov et al. 2012, Akbari et al. 2014, Wang et al. 2014). In addition, all research proved that there is a nonlinear relationship between specific energy and the back rake angle. Coudyzer and Richard (2005) reported an increase in specific energy up to five-fold when increasing the back rake angle from *10°* to*60°*. Besides, they deduced that the side rake angle has a minor effect on specific energy up to 45 degrees. Rajabov et al. (2012) performed experiments regarding influence of the back rake and side rake angles on the cutting forces at both atmospheric and confining pressure. The outcome indicated that for constant confining pressure, specific energy increases with an increase in the back rake angle. Likewise, they observed that the effect of the side rake angle on Mechanical Specific

Energy is negligible between 0- and 30-degree side rake angles compared to angle values between 30 and 60 degrees and could increase by three-fold when the side rake angle increases from 30 to 60 degrees. However, such values of side rake angles are not applicable in PDC bits with circular cutters unless non-circular cutters with in-built side rake angles (similar to cutters introduced in the work by Liu et al. (2019)) are implemented during manufacturing.

Cutting area and wear height. The most complex and important part of PDC cutter modeling is studying the effect of the cutter-rock interface on full-scale bits performance because the contact area instantaneously changes during drilling. In addition to the axial force from the weight on bit, the contact area between the cutter and rock depends on the wear condition of the cutter. Considerable experimental research has been done to investigate the effects of the cutting area on the applied forces (Glowka 1989, Akbari et al. 2014, Goshouni and Richard 2008, Wang et al. 2014). The lapping effect of the adjacent cutter on the surface area was investigated both experimentally and theoretically (Huang et al. 2017, Chen et al. 2019, Zhu et al. 2020). Single cutter experiments indicated that there is a linear relationship between forces and the cutting area (Wang et al. 2014); while in the case of overlapping cutters there is a power relationship between the axial and cutting forces with the contact area (Liang et al. 2014).

All modeling efforts concerning the rate of penetration should include a continuous computation of the cutter wear state during drilling to optimize the drilling operation and decide when to terminate the PDC bit run. A reliable cutter wear model could be utilized to build force models on cutters and successively implement such a concept in designing cutter placement during the manufacturing of bits (Pryhorovska 2017, Ai et al. 2018). Extensive research on blunt and new cutters pinpoints the importance of changes in the geometry of cutters on the force state during the cutting of rock. Detournay et al. (1992, 2008, 2000) have provided a thorough mathematical representation of the relationship between the frictional surface area and force distribution. As cutters wear out, the frictional contact area develops below cutters and dominates the force distribution on cutters and general bit performance (Zijsling 1987, Zhou and Detournay 2014, Detournay et al. 2008, Rostamsowlat et al. 2019, Dagrain and Richard 2006).

Rock drillability. In addition to all the necessary design criteria, rock mechanical properties are impossible to control, and all design parameters and applied drilling parameters should be decided to overcome variant rock drillability. Rock drillability changes during drilling are based on changes in lithology, porosity, permeability, compaction, and the cementation material of rock. There is little research on rock drillability but almost all previous studies mentioned here performed experimental and analytical investigations of different rock types. A summary of rock properties (such as the rock friction angle, shear stress, uniaxial and confined compressive stress) of the data utilized in this study is provided in Table 1.

Sinor and Warren (1989) developed a drag bit wear model based on experiments for three rock types i.e., Carthage limestone, Berea sandstone, and Catoosa shale. Wang et al. (2014) performed experiments on four different rocks (Shale, Marble, Granite, and Limestone) and defined drillability ranges from 5.0 to 7.0. In this study, the effect of rock drillability is acknowledged by parameter K (Wang et al. 2014, Liang et al. 2014) and plugged in the cutter force formulations.

An intensive survey of the literature signifies the importance of parameters such as back rake angle, contact area, cutter worn height, frictional contact area, rock drillability, and differential pressure on the performance of cutter-rock interaction. On the other hand, the influence of parameters such as cutting speed and side rake angle are considered to be negligible (Che et al. 2016). Each of the studies focused on a limited number of the mentioned parameters. The novelty of the present study is that it develops two correlations to estimate axial force, F_a, (force that is parallel to the axis of the bit) and cutting force, F_c, (force perpendicular to the axis of the bit and in direction of rotation of cutter) considering all design, operational and rock parameters. Experimental data from the literature are collected and implemented in nonlinear regression analysis using optimization algorithms.

Table 1—Rock physical properties for for data used in this study.

Reference	Rock Name	Bulk Density (gr/cc)	Porosity (%)	UCS (kpsi)	Poisson's Ratio	Young's Modulus (Mpsi)
Rajabov et al. 2012	Carthage Marble	2.63	1-2	9-12	0.27	4-5
	Torrey Buff Sandstone	2.54	7.9	9-11	0.22	1.5-1.6
	Mancos Shale	2.47	16	5-7	0.2	4.6
Glowka 1989	Berea Sandsone	-	-	7.1	-	-
	Sierra White Granite	-	-	21.5	-	-
	Tennessee Marble (Holton limestone)	-	-	17.8	-	-
Akbari et al. 2014 Akbari et. Al.	Carthage Marble			14.48		
Richard et al. 2010	Fontenoille Sandstone	-	-	13.775	-	-
	Moka Limestone	-	-	9.425	-	-
	Lens Limestone	-	-	4.35	-	-
	Voges Sandstone	-	20	2.32	-	-
	Nurabup Sandstone	-	41	1.16	-	
	MC Field Sandstone	-	24.5	1.015	-	-
Majidi et al. 2011	Indiana Limestone	-	11-16	7	-	-
	Carthage Marble	-	1-2	9-11.7	-	-
Wang et al. 2014					Tensile Strength (kpsi)	
	Shale	-	-	9.764	0.81	
	Marble	-	-	12.294	0.90	
	Granite	-	-	13.656	1.017	
	Limestone	-	-	15.013	1.141	

The dashes indicate that data are not available for that rock in the mentioned reference.

Experimental data

For this study two sets of separate experimental data were collected from the literature to regress correlations for axial and cutting force. Experimental data covered force values for both new and dull circular cutters. Data collected and applied in the regression include cutter diameter, cutting area, cutter wear flat (or frictional surface) area, back rake angle, cutter wear height, rock drillability, and differential pressure (see Figure 1). Besides utilizing geometrical analysis, the cutting area was calculated from the depth of cut that was measured during the experiments in the literature. For those works that did not report a value of rock drillability, an estimate of drillability was calculated from equations in the publication by Liang et al. (2014) based on the data provided for rock cutting utilizing new cutter tests. For new cutters, the frictional surface area below the cutter is considered zero and for dull cutters, values reported in the literature are applied in the calculations. However, the number of studies examining cutters-rock interaction exceeds those cited here. Some necessary parameters were not reported in a few studies and the data package was not clear enough to be implemented.

A summary of experimental data points from numerous studies is presented in Table 2. In total, 779 and 654 data points were collected for cutting and axial force, respectively. The back rake angle in the

experiments ranges from 0 to 40 degrees, fluid confining pressure was between 0 to 450 psi, cutter sizes from 12.7 mm to 19 mm were utilized and various rock types with different mechanical and petrophysical properties were implemented for testing. Tables 3 and 4 represent the statistical values of data for axial and cutting forces.

Table 2—Summary of experimental data implemented in regression; F_a, Axial Force; F_c, Cutting Force.

Reference	No. of data in Fn, Fc	Cutter Condition	Cutter Size (mm)	Back Rake Angle (°)	Pressure Difference (psi)
Rajabov et al. 2012	40, 117	New	13	10, 20, 30, 40	0, 250, 500
Glowka 1989	403, 403	New, Dull	12.7, 19	20	0
Akbari et. al. 2014	64, 67	New	13, 16	20	450
Richard et al. 2010	0, 50	New	13, 19	15	0
Majidi et al. 2011	54, 54	New	13	15	0, 50, 150, 250
Wang et al. 2014	93, 88	New	13	5, 10, 15, 20, 25	0

Table 3—Statistical summary of experimental data employed in regression of F_n (Number of observations 654).

Variable	Mean	Standard Deviation	Minimum	Maximum
Axial Force (N)	2124.7	1957.33	59.16	7893.36
Cutter Diameter (mm)	---	---	12.7	19.05
Cutting Area (mm^2)	9.19	8.08	0.1	49.5
Wear Flat Area (mm^2)	10.78	10.58	0	25.8
Back Rake Angle (deg)	---	---	5	40
Cutter Wear Height (mm)	0.68	0.65	0	1.69
Rock Drillability, K (dimensionless)	5.46	0.94	3.2	7.78
Differential Pressure (psi)	52.67	136.81	0	450

Table 4—Statistical summary of experimental data employed in regression of F_c (Number of observations 779).

Variable	Mean	Standard Deviation	Minimum	Maximum
Cutting Force (N)	1382.48	1224.54	11.41	5747.19
Cutter Diameter (mm)	---	---	12.7	19.05
Cutting Area (mm^2)	8.53	7.56	0.11	37.92
Wear Flat Area (mm^2)	9.05	10.47	0	25.8
Back Rake Angle (deg)	---	---	5	40
Cutter Wear Height (mm)	0.57	0.65	0	1.69
Rock Drillability, K (dimensionless)	5.36	1.07	3.2	7.78
Differential Pressure (psi)	78.32	156.88	0	500

Regression Analysis

Experimental studies with different cutter sizes on numerous rock types and under varied experimental conditions have revealed that cutting and axial forces are related to the back rake angle, cutting and wear flat area, rock drillability, differential pressure, and cutter worn height through some simple linear and nonlinear equations. Table 5 summarizes the mathematical formulation of the basis regression functions based on the

rock-cutter interface parameters. Each basis function suggests a transformation for each of the objective parameters. The basis functions for back rake angle, wear flat area, differential pressure, and wear height are proposed in such a way that if the objective parameter is zero then the parameters do not influence the force values. Besides, if the cutting area is zero then forces become zero as well. Therefore, correlations are valid if drilling continues for the applied parameters. The coefficient λ_i in these basis functions is limited to some values based on the experimental outcomes and such bounds are tabulated in Table 5.

Table 5—Proposed basis regression functions based on experimental observations for F_a and F_c.

Parameter	Basis Function	Multiplier Bounds	References
Back Rake Angle (θ)	$e^{\lambda_1 \sin(\theta)}$	$\lambda_1 \geq 0.5$	Wang et al. 2014, Liang et al. 2014, Akbari and Miska 2016, Rajabov et al. 2012
Cutting Area (A_{cut})	$A_{cut}^{\lambda_2}$	$0.4 \leq \lambda_2 \leq 0.9$	Glowka 1989, Akbari et al. 2014, Wang et al. 2014, Liang et al. 2014, Rajabov et al. 2012, Akbari and Miska 2017, Majidi et al. 2011
Wear Flat Area (A_{wear})	$e^{\lambda_3 (A_{wear})^{\lambda_4}}$	$0.1 \leq \lambda_3 \leq 0.3$ $0.1 \leq \lambda_4 \leq 1.0$	Glowka 1989; Appl et al. 1993
Rock Drillability (K)	K^{λ_5}	$1.0 \leq \lambda_5 \leq 4.0$	Wang et al. 2014
Confining Pressure (ΔP)	$e^{\lambda_6 (\Delta P)^{\lambda_7}}$	$0.2 \leq \lambda_6 \leq 1.4$ $0.1 \leq \lambda_7 \leq 0.4$	Rafatian et al. 2009, Rajabov et al. 2012, Akbari et al. 2014, Akbari and Miska 2017, Zijsling 1987
Cutter Wear Height (h_w)*	$e^{\lambda_8 \left(\frac{h_w}{OD\cos(\theta)}\right)}$	$1.0 \leq \lambda_8 \leq 2.0$	Glowka 1989, Appl et al. 1993

λ_i could be either α_i or β_i utilized in axial and cutting force.

*OD stands for cutter diameter in mm.

As it is demonstrated in Table 4, each of the functions entails one or two multipliers which are bounded to some values based on the observations for every single parameter reported in the literature. The basis function for wear flat area and cutter wear height were configured in such a way that if cutter status is new then these parameters do not affect force values.

Two equations were assembled utilizing basis functions to estimate axial and cutting forces. The proportionality of the basis functions switched to equality by incorporating proportionality constants (α_0,β_0). In the following correlations, the constants α_0 and β_0 carry the influence of those parameters such as cutting speed, chamfer, and side rake angles because there are not enough experimental data to include them in the regression process.

$$F_a = e^{\alpha_0}\left(e^{\alpha_1 \sin(\theta)}\right)\left(A_{cut}^{\alpha_2}\right)\left(e^{\alpha_3 (A_{wear})^{\alpha_4}}\right)\left(K^{\alpha_5}\right)\left(e^{\alpha_6 (\Delta P)^{\alpha_7}}\right)\left(e^{\alpha_8 \left(\frac{h_w}{OD\cos(\theta)}\right)}\right)$$

$$F_c = e^{\beta_0}\left(e^{\beta_1 \sin(\theta)}\right)\left(A_{cut}^{\beta_2}\right)\left(e^{\beta_3 (A_{wear})^{\beta_4}}\right)\left(K^{\beta_5}\right)\left(e^{\beta_6 (\Delta P)^{\beta_7}}\right)\left(e^{\beta_8 \left(\frac{h_w}{OD\cos(\theta)}\right)}\right)$$

To perform regression, different optimization techniques such as the genetic algorithm, deep learning, particle swarm optimization, and *fmincon* function of MATLAB were applied. The scope of all techniques was to minimize the objective function defined in the following equation. Constrained optimization was performed based on the upper and lower bounds and the output solution for the objective function is valid for these intervals. Optimization of the objective function resulted in R -squared (coefficient of determination of the percentage of variation in dependent variables explained by the regression) values of 0.7659 and 0.9387 for axial and cutting forces, respectively. Further details of regression are provided in Tables 6 and 7. R -square is a measure of the exactness of the regression, but F -factor presents a hypothesis test for the entire regression. This test indicates how strongly the dependent variable is related to the independent parameters. Here the critical F values for the axial and cutting forces based on the degree of freedom are equal to *2.1442* while F values from the regression are *1652.53* and *505.576* for axial and cutting forces, respectively. The

comparison of critical F values with values from the regression indicates that there exists a hypothesis that confirms a relationship between force values and the independent cutter, rock, and operational (confining pressure) parameters.

$$J = \sum_{i=1}^{N} \left(\frac{F_{\text{experiment}_i} - F_{\text{model}_i}}{F_{\text{experiment}_i}} \right)$$

Table 6—Regression analysis for correlation of cutting force.

Source	Sum of Squares	Degree of freedom	Mean of Square	F-factor
Regression (F_c)	745.727	6	149.145	505.576
Residual	228.083	772	0.295	
Total	973.810	778	1.251	

Table 7—Regression analysis for correlation of axial force.

Source	Sum of Squares	Degree of freedom	Mean of Square	F-factor
Regression (F_a)	4736.6	6	789.434	1652.53
Residual	309.08	647	0.4771	
Total	5045.68	653	7.7269	

Deep Learning Regression

In addition to regression analysis by numerous techniques such as the genetic algorithm, particle swarm optimization and *fmincon* function of MATLAB, deep learning techniques were performed on data to correlate axial and cutting forces to cutter design parameters, rock drillability, and differential pressure. Therefore, a neural network model was developed and evaluated using Keras for a regression.

The rectifier activation function was used for input and the hidden layers. Three layers with 100, 200, and 100 neurons were assembled to make up the networks. The efficient ADAM optimization algorithm was used, and a mean squared error loss function was instrumented to evaluate the performance of the model.

As the amount of data point is not high enough to run the usual regression on data points, the plan was to apply all data as input to the network. Therefore, the repeated k-fold cross-validation procedure was implemented, and the result is designed to provide a more accurate estimate. The k-fold cross-validation procedure divides a limited dataset into K non-overlapping folds (as usual a good default for k was chosen as 10 folds). Each of the K folds are given an opportunity to be used as a held back test set, whilst all other folds collectively are used as a training dataset (Chollet 2018).

Finally, Figures 2 and 3 exhibit force values from the experiment and calculated values from regressed models and deep learning estimation. It is shown there is a good correlation between regressed and experimental data points. The discrepancy in some data points originates from the fact that none of the experiments reported in the literature examined all design and operational parameters (parameters introduced in this study for regression). Besides, the estimated values by nonlinear regression and deep learning follow the same pattern and have nearly identical values.

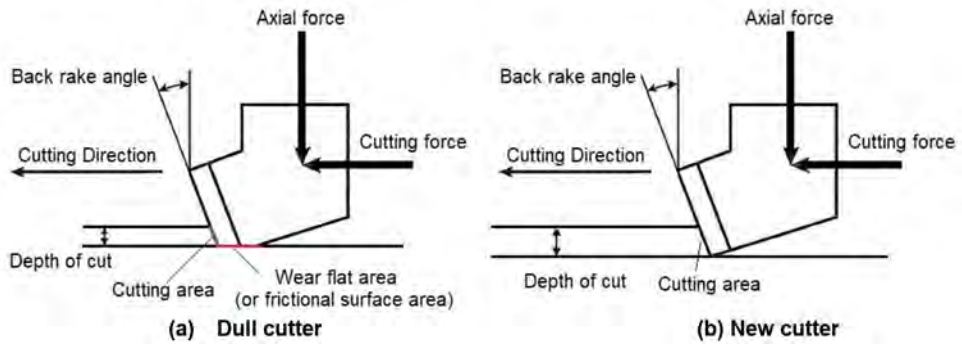

Figure 1—Geometry parameters for dull and new cutters.

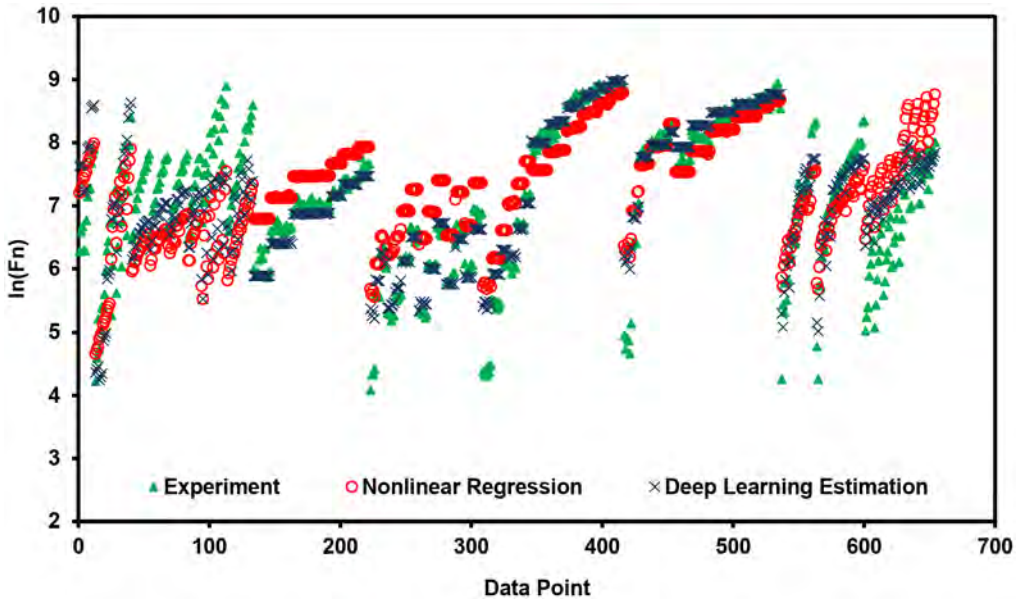

Figure 2—Scatter plot of experimental and model data for axial force.

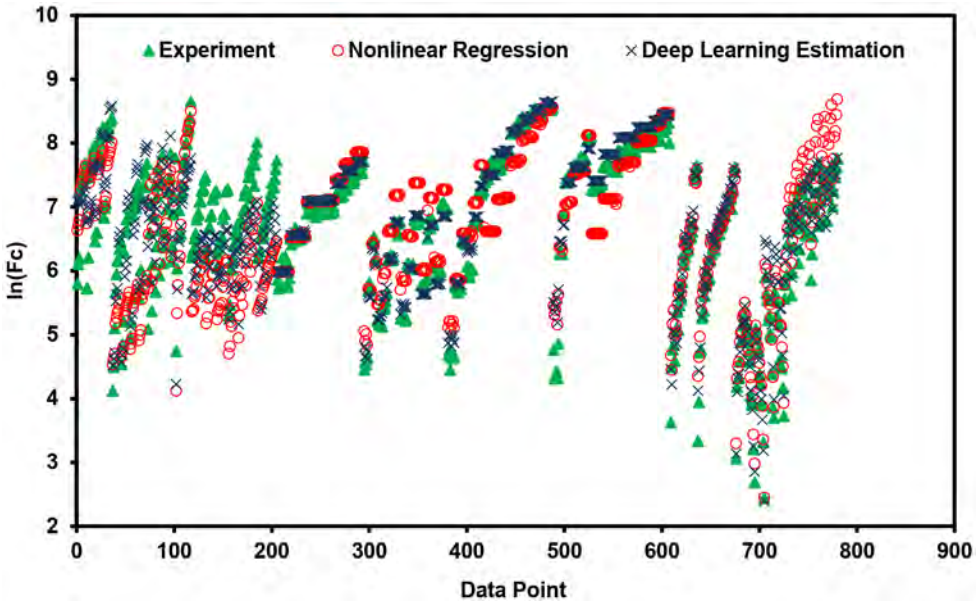

Figure 3—Scatter plot of experimental and model data for cutting force.

ANOVA Analysis

In order to assess the relative significance of each parameter, *ANOVA* (**a**nalysis **o**f **v**ariance) can be implemented along with regression techniques. ANOVA introduces a hypothesis test (*t-test*) which determines how much each parameter contributes to the prediction of the value of the dependent variable. The ANOVA analysis for axial and tangential forces was performed using MATLAB and STATA software and the results are tabulated in Tables 8 and 9. As it is demonstrated by values of *t-stat*, the cutting area, rock drillability and differential pressure have the greatest influence (more than 70%) on axial and cutting forces. Furthermore, *P* -values for each variable are less than the conventional value of significance of *0.05* which confirms the hypothesis of correlation between variables.

Table 8—Regression coefficients of axial force along with t-test and P- values.

Cutting Force (F_a)	Coefficient	Standard Error	*t-test*	*P-value*	95% Confidence Interval	
α_0	0.0					
α_1	1.2826	0.3836	3.34	0.001	0.5294	2.0358
α_2	0.4524	0.0288	15.7083	0.0	0.4308	0.4776
α_3*	0.1	---	---	---	---	---
α_4**	0.7055	---	---	---	---	---
α_5	3.2531	0.0714	45.5616	0.0	3.0342	3.5148
α_6	0.2958	0.0603	4.9054	0.002	0.2	0.3044
α_7***	0.4	---	---	---	---	---
α_8	1.0	---	---	---	---	---

*As lower bound was set for the variable, ANOVA is not available.

**Coefficient considered as constant for ANOVA analysis.

***As upper bound was set for the variable, ANOVA is not available

Table 9—Regression coefficients of axial force along with *t-test* and *P*-values.

Cutting Force (F_c)	Coefficient	Standard Error	*t-test*	*P-value*	95% Confidence Interval	
β_0	0.2469	0.1821	1.3558	0.004	0.1632	0.8782
β_1	0.5237	0.0216	24.2453	0.001	0.50	0.7370
β_2	0.7454	0.0562	13.2633	0.0	0.6013	0.8347
β_3*	0.1	---	---	---	---	---
β_4**	0.6432	---	---	---	---	---
β_5	2.6821	0.0947	28.3220	0.0	2.4564	2.8283
β_6	0.5173	0.0387	13.3669	0.0	0.3789	0.5310
β_7***	0.4	---	---	---	---	---
β_8	1.0	---	---	---	---	---

*As lower bound was set for the variable, ANOVA is not available.

**Coefficient considered as constant for ANOVA analysis.

***As upper bound was set for the variable, ANOVA is not available

Conclusion

Advanced real-time drill bit modeling requires knowledge of the forces and stresses at the bit cutters. Furthermore, optimum selection of cutter design and placement depends on the distribution of forces and stress in the rock. In order to develop correlations for axial and cutting forces, more than 700 experimental data points were collected, and regression analysis was performed to correlate equations for axial and cutting forces by minimizing an objective function. ANOVA analysis of the data and correlations proposed a strong relationship between axial and cutting forces with the cutting area, rock drillability and differential pressure. In these correlations the influence of parameters such as chamfer angle, side rake angle and cutting speed were not included because there were not enough experimental observations, and this could be the scope for future research. Furthermore, research has indicated that these parameters have a minor effect on axial and cutting forces.

The core idea behind this study was to develop techniques for real-time drill bit modeling using along string measurement data by wired drill pipes. There is a stream of downhole drilling data being continuously recorded using along string measurement recorders. These data such as weight and torque on bit, rotary speed, fluid pressure, temperature, and acceleration at bit provide information about downhole dynamics. By implementing coupled models of rock-bit interaction, which have been performed in this study, also using data analytics techniques reliable conclusions could be drawn to diagnose drilling events and symptoms in real-time operations.

Among the problems that could be anticipated, evaluated, and administered are those that have direct relation to data recorded by an along string measurement system. Further research is planned to take advantage of such an approach to diagnose real-time faults and symptoms using wired pipe for numerous phenomena. These include annular pack off, formation losses or kicks, stick and slips of the drillstring, bit whirling and torsional vibration or even developing an algorithm for continuous automatic dull grading of the bit during drilling operations.

Acknowledgement

This research is a part of BRU21 – NTNU Research and Innovation Program on Digital and Automation Solutions for the Oil and Gas Industry at the Norwegian University of Science and Technology (www.ntnu.edu/bru21).

References

Ai, Z., Han, Y., Kuang, Y., Wang, Y., Zhang, M. 2018. Optimization Model for Polycrystalline Diamond Compact Bits Based on Reverse Design. *Adv in Mech Eng* **10**: 1–12. https://doi.org/10.1177/1687814018781494.

Akbari, B., Miska, S., Yu, M., Ozbayoglu, M. 2014. Experimental Investigations of The Effect of The Pore Pressure on The MSE and Drilling Strength of a PDC Bit. Presented at the SPE Western North American and Rocky Mountain Joint Meeting, Denver, Colorado. SPE-169488-MS. https://doi.org/10.2118/169488-MS.

Akbari, B., Miska, S. Z., Yu, M., Rahmani, R. 2014. The Effects of Size, Chamfer Geometry, and Back Rake Angle on Frictional Response of PDC Cutters. Presented at the 48th Rock U.S. Mechanics/Geomechanics Symposium, Minneapolis, Minnesota. ARMA-2014-7458.

Akbari, B., Miska, S. 2016. The Effects of Chamfer and Back Rake Angle on PDC Cutters Friction. *Journal of Natural Gas Science and Engineering* **35 (Part A)**: 347–353. https://doi.org/10.1016/j.jngse.2016.08.043.

Akbari, B., Miska, S. Z. 2017. Relative Significance of Multiple Parameters on The Mechanical Specific Energy and Frictional Responses of Polycrystalline Diamond Compact Cutters. *ASME. J Energy Resour Technol* **139**(2): 022904.

Appl, F. C., Wilson, C., Lakshman, I. 1993. Measurement of Forces, Temperatures and Wear of PDC Cutters in Rock Cutting. *Wear* **169**: 9–24. https://doi.org/10.1016/0043-1648(93)90386-Z.

Che, D., Zhang, W., Ehmann, K. F. 2016. Rock-cutter interactions in linear rock cutting. 11th International Manufacturing Science and Engineering Conference - Blacksburg, United States. doi:10.1115/MSEC20168510.

Chen, P., Miska, S., Ren, R., Yu, M., Ozbayoglu, E., Takach, N. 2018. Poroelastic Modeling of Cutting Rock in Pressurized Condition. *J Pet Sci Eng*. **169**: 623–635. H ttps://doi.org/10.1016/j.petrol.2018.06.009.

Chen, P., Meng, M., Miska, S., Yu, M., Ozbayoglu, E., Takach, N. 2019. Study on Integrated Effect of PDC Double Cutters. *J Pet Sci Eng*. **178**. 1128–1142. 10.1016/j.petrol.2019.04.024">https://doi.org/10.1016/j.petrol.2019.04.024.

Chollet, F. 2018. Deep Learning with Python, second edition. Manning Publications Co., New York.

Coudyzer, C., Richard, T. 2005. Influence of The Back and Side Rake Angles in Rock Cutting. AADE-05NTCE-75 In Proceedings of National Technical Conference and Exhibition held at the Wyndam Greenspoint in Huston, Texas.

Dagrain, F., Richard, T. 2006. On The Influence of PDC Wear and Rock Type on Friction Coefficient and Cutting Efficiency. Eurock. Liège, Belgium.

Detournay, E., Defournay, P. 1992. A Phenomenological Model for The Drilling Action of Drag Bits. *Int J Rock Mech Sci & Geomech Abstr* **29**(1): 13–23. https://doi.org/10.1016/0148-9062(92)91041-3.

Detournay, E., Richard, T., Shepherd, M. 2008. Drilling Response of Drag Bits: Theory and Experiment. *Int J Rock Mech Min Sci*. **45** (8): 1347–1360. https://doi.org/10.1016/j.ijrmms.2008.01.010.

Detournay, E., Atkinson, C. 2000. Influence of Pore Pressure on The Drilling Response in Low Permeability Shear Dilatant Rocks. *Int J of Rock Mech Min Sci* **37** (7): 1091–1101. https://doi.org/10.1016/S1365-1609(00)00050-2.

Dagrain, F., Detournay, E., Richard, T. 2001. Influence of Cutter Geometry in Rock Cutting. Presented at the DC Rocks 2001, The 38th Symposium U.S. on Rock Mechanics (USRMS), Washington, D.C., July 2001. ARMA-01-0927.

Glowka, D. A. 1989. Use of Single-Cutter Data in The Analysis of PDC Bit Designs: Part 1- Development of a PDC Cutting Force Model. *J Pet Technol* **41** (08): 797–849. SPE-15619-PA. https://doi.org/10.2118/15619-PA.

Glowka, D. A. 1989. Use of Single-Cutter Data in The Analysis of Pdc Bit Designs: Part 2- Development and Use of The Pdc Wear Computer Code. *J Pet Technol* **41** (08): 850–859. SPE-19309-PA. https://doi.org/10.2118/19309-PA.

Goshouni, M., Richard, T. 2008. Effect of Back Rake Angle and Groove Geometry in Rock Cutting. Presented at the ISRM International Symposium - 5th Asian Rock Mechanics Symposium, Tehran, Iran. ISRM-ARMS5-2008-027.

Grima, M. A., Miedema, S. A., {van de} Ketterij, R. G., Yenigül, N. B., {van} Rhee, C. 2015. Effect of High Hyperbaric Pressure on Rock Cutting Process. *Engineering Geology* **196** (28): 24–36. https://doi.org/10.1016/j.enggeo.2015.06.016.

Huang, Z., Ma, Y., Li, Q., Xie, D. 2017. Geometry and Force Modeling, and Mechanical Properties Study of Polycrystalline Diamond Compact Bit Under Wearing Condition Based on Numerical Analysis. *Adv Mech Eng* **9**: 1–15. ttps://doi.org/10.1177/1687814017702080.

Ledgerwood, L. W. 2007. PFC Modeling of Rock Cutting Under High Pressure Conditions. Presented at the 1st Canada - Rock U.S. Mechanics Symposium, Vancouver, Canada. ARMA-07-063. doi:10.1201/NOE0415444019-c63.

Liang, E., Wang, J., Zhou, L., Wang, L. 2014. The Analysis of Force on PDC Cutter. *In: Energy Materials* 2014. Springer, Cham. 781–787. https://doi.org/10.1007/978-3-319-48765-6_96.

Liu, J., Zheng, H., Kuang, Y., Xie, H., Qin, C., 3D Numerical Simulation of Rock Cutting of an Innovative Non-Planar Face PDC Cutter and Experimental Verification. *Appl Sci*. **4372**. doi:10.3390/app9204372.

Majidi, R., Miska, S. Z., Tammineni, T. 2011. PDC single cutter: the effects of depth of cut and RPM under simulated borehole conditions Wiertnictwo, *Nafta, Gaz. T*. **28**, z. 1-2: 283–295.

Pryhorovska, T. O. 2017. Study on Rock Reaction Force Depending on PDC Cutter Placement. *Mach Sci Tech* **21**: 37–66. https://doi.org/10.1080/10910344.2016.1260429.

Rafatian, N., Miska, S., Ledgerwood, L. W. Ahmed, R., Yu, M., Takach, N. 2009. Experimental Study of MSE of a Single PDC Cutter Interacting with Rock Under Simulated Pressurized Conditions. *SPE Drill & Compl* **25** (01): 10–18. SPE-119302-PA. https://doi.org/10.2118/119302-PA.

Rajabov, V., Miska, M., Mortimer, L., Yu, M., Ozbayoglu, E. 2012. The Effects of Back Rake and Side Rake Angles on Mechanical Specific Energy of Single PDC Cutters with Selected Rocks at Varying Depth of Cuts and Confining Pressures. Presented at the IADC/SPE Drilling Conference and Exhibition, San Diego, California, USA, March 2012. SPE-151406-MS. https://doi.org/10.2118/151406-MS.

Richard, T., Coudyzer, C., Desmette, S. 2010. Influence of Groove Geometry and Cutter Inclination in Rock Cutting. Presented at the 44th Rock U.S. Mechanics Symposium and 5th U.S.-Canada Rock Mechanics Symposium, Salt Lake City, Utah. ARMA-10-429.

Rostamsowlat, I., Richard, T., Evans, B. 2019. Experimental Investigation on The Effect of Wear Flat Inclination on The Cutting Response of a Blunt Tool in Rock Cutting. *Acta Geotech*. **14**: 519–534. https://doi.org/10.1007/s11440-018-0674-1.

Sinor, A., Warren, T. M. 1989. Drag Bit Wear Model. *SPE Drill Eng* **4** (02): 128–136. SPE-16699-PA. https://doi.org/10.2118/16699-PA.

Wang, J., W., Deyonga, Z., Renqinga, H. 2014. Experimental Study on Force of PDC Cutter Breaking Rock. *Procedia Engineering*. **73**: 258–263. https://doi.org/10.1016/j.proeng.2014.06.196.

Zhu, X., Deng, Z., Liu, W. 2020. Experimental Study on Energy Consumption of Rock Cutting Under Different Groove Geometry. *Geotechnical Testing Journal*. **43** (1): 151–170. https://doi.org/10.1520/GTJ20180214.

Zhou, Y., Detournay, E. 2014. Analysis of The Contact Forces on a Blunt PDC Bit. Presented at the 48th Rock U.S. Mechanics/Geomechanics Symposium, Minneapolis, Minnesota. ARMA-2014-7351.

Zijsling, D. H. 1987. Single Cutter Testing - A Key for PDC Bit Development. Presented at the SPE Offshore Europe, Aberdeen, United Kingdom, September 1987. SPE-16529-MS. https://doi.org/10.2118/16529-MS.